Thin Solid Films 520 (2012) 7049–7053

Contents lists available at SciVerse ScienceDirect

Thin Solid Films

journal homepage: www.elsevier.com/locate/tsf

Effect of conducting polypyrrole on the transport properties of carbon nanotube yarn

Javad Foroughi [a,b,*], Bahram Kimiaghalam [b], Shaban Reza Ghorbani [c], Farzad Safaei [b], Mehran Abolhasan [d]

[a] ARC Centre of Excellence for Electromaterials Science, Intelligent Polymer Research Institute, University of Wollongong, Wollongong, NSW 2519, Australia
[b] Information and communication Technology Research Institute, University of Wollongong, Wollongong, NSW 2519, Australia
[c] Department of Physics, Hakim Sabzevari University, P.O. Box 397, Sabzevar, Iran
[d] Faculty of Engineering and IT University of Technology Sydney, Sydney, NSW Australia

ARTICLE INFO

Article history:
Received 27 July 2011
Received in revised form 17 July 2012
Accepted 24 July 2012
Available online 28 July 2012

Keywords:
Carbon nanotube yarn
Conducting polymer
Polypyrrole
Electrical conductivity
Vapor phase polymerization

ABSTRACT

Experiments were conducted to measure the electrical conductivity in three types of pristine and carbon nanotube-polypyrrole (CNT-PPy) composite yarns and its dependence on over a wide temperature range. The experimental results fit well with the analytical models developed. The effective energy separation between localized states of the pristine CNT yarn is larger than that for both the electrochemically and chemically prepared CNT-PPy yarns. It was found that all samples are in the critical regime in the insulator–metal transition, or close to the metallic regime at low temperature. The electrical conductivity results are in good agreement with a Three Dimensional Variable Range Hopping model at low temperatures, which provides a strong indication that electron hopping is the main means of current transfer in CNT yarns at $T<100$ K. We found that the two shell model accurately describes the electronic properties of CNT and CNT-PPy composite yarns in the temperature range of 5–350 K.

1. Introduction

Carbon nanotubes (CNTs) have great potential for conducting and sensing applications owing to their unique, tunable electrical properties [1–5]. The excellent conductivities of CNTs and their ability to carry very high current density, along with their high thermal conductivity, chemical stability and mechanical strength, make CNTs uniquely promising for a broad range of applications, including building blocks for nanoscale electronic devices, microsensors for bio-agents and chemicals, artificial muscle and power cables for space shuttles [6–10]. In addition, CNTs have been considered a most promising nanomaterial due to their small diameter of 1–2 nm for single-walled nanotubes (SWNT) and 10–50 nm for multi-walled nanotubes (MWNT) [11]. However, individual carbon nanotubes are hard to manipulate and undersized for many applications. In 2004, a method of producing yarns from aligned MWNT forests was invented that expanded the application of CNTs [2].

The electrical resistivity of individual CNTs has been measured under ballistic conductions to be as low as $10^{-6}\,\Omega$ cm for SWNT and $3\times10^{-5}\Omega$ cm for MWNT, respectively [12–15]. These measurements indicate that CNTs may be better conductors than metals such as copper at room temperature. However, in most cases, due to the presence of various defects or impurities formed during the CNT growth, the conductivities of individual CNTs are often much lower than those under ballistic conduction with nanotubes free of defects [16,17]. The electron transport in CNT assemblies such as yarn is also different from that in individual nanotubes. It has been reported that SWNT fibers, either synthesized directly by vertical floating chemical vapor deposition methods [1,4] or extruded from a super-acid suspension [3], exhibit room-temperature resistivities in the range of 1×10^{-4} to $7\times10^{-4}\,\Omega$ cm, which is nearly 100 times higher than the resistivities of single nanotubes. The resistivities of MWNT yarns are typically one or two orders of magnitude higher than that of SWNT yarn [2,5]. Such large differences between single nanotubes and yarn assemblies may arise from a high impurity content such as amorphous carbon and catalytic particles in the yarn, which may profoundly affect electron transport by causing significant scattering, and contact resistances between nanotubes [18]. There have been several studies concerned with enhancing the electrical properties of CNT assemblies, [19] however, there are none dealing with improvement of the electrical properties of CNT yarn. We felt that adding conducting material into the structure of the CNT yarn may enhance its electrical properties.

Conducting polymers are good candidates for this purpose because their π orbital electrons are easily de-located for contribution to conduction. There have been several attempts to measure transport properties of conjugated polymers such as film or fibers [20,21]. The low temperature transport in doped single polyacetylene fibers and polypyrrole (PPy) nanotubes has been studied [11,22] and the tunneling transport mechanism has also been considered [23]. Recently, we have reported the transport properties and electrical conductivity of conducting polypyrrole fibers and film [24] and, following on from this work, we report here a method to improve the electrical properties of CNT yarn.

* Corresponding author at: ARC Centre of Excellence for Electromaterials Science, Intelligent Polymer Research Institute, University of Wollongong, Wollongong, NSW 2519, Australia. Fax: +61 2 42213114.
E-mail address: foroughi@uow.edu.au (J. Foroughi).

0040-6090/$ – see front matter © 2012 Elsevier B.V. All rights reserved.
http://dx.doi.org/10.1016/j.tsf.2012.07.108

The electrical conductivity of both pristine and CNT composite yarns has been studied and the results strongly suggest that the main current carrying regime is Three Dimensional Variable Range Hopping (3D-VRH). In addition, the effective energy separation between localized states of the pristine CNT yarn is larger than that for both the electrochemically and chemically prepared CNT-PPy yarns. They show critical behavior in the insulator–metal transition at lower temperatures.

2. Experimental details

MWNT forest was synthesized by catalytic chemical vapor deposition using acetylene gas as the carbon source [2]. Carbon nanotubes in the 300 μm tall forest typically had diameters of about 10 nm. The yarns (pristine CNT) were drawn from the forest by pulling and twisting as described by Zhang et al [2]. The CNT-PPy composite yarn was prepared by electrochemical (Electrochem. CNT-PPy) and chemical (Chem. CNT-PPy) polymerization of pyrrole on the surface of the MWNT yarn. Chem. CNT-PPy yarns were developed by chemical polymerization of pyrrole through vapor phase polymerization. A length of CNT yarn was fixed into a frame which was dipped into Fe.*p*TS (oxidant/dopant) solution for 10 min. The CNT yarn coated with Fe.*p*TS was then dried at 60 °C for 30 min. The dried CNT/Fe.*p*TS yarn was placed in a chamber containing monomer (pyrrole) for 12 h at room temperature. Polypyrrole then formed on and within the CNT yarn. The CNT-PPy yarn was washed with methanol to remove salts and/or monomer from the sample. As-prepared CNT-PPy yarn was dried at room temperature and was used for further experiments. A comparison of the weight of sample before and after polymerization indicated that the weight fraction of the PPy in the CNT-PPy yarn was ~8 wt.%. Polypyrrole was incorporated into the CNT yarn by anodic oxidation of pyrrole monomer. CNT yarns were attached to a frame which was used as the anode and a stainless steel plate as the cathode. The electrolytic cell contained 0.10 M Fe.*p*TS, 0.10 M pyrrole and water. The polymerization was carried out galvanostatically using a constant current of 0.10 mA/cm^2 for 6 h at −0 °C. The geometric surface area of a 20 μm diameter yarn was used to estimate the surface area. The resultant yarn was washed several times with acetone, and then allowed to dry for 24 h in air at room temperature. A comparison of the weight of sample before and after polymerization indicated that the weight fraction of PPy in the electrochemical prepared CNT-PPy yarn has ~74 wt.% [25].

A Leica Stereoscan 440 Scanning Electron Microscope (SEM) with tungsten filament using 20 kV beam energy was used for morphological studies of the yarns. Electrical transport of the carbon nanotubes and CNT-PPy yarns was characterized by a standard four probe technique (Quantum Design PPMS). All measured yarns were placed onto MgO substrate and four Au wires were attached sample using silver paste. The dependence of conductivity (σ) on temperature (T) was measured by sweeping the temperature from 350 K to 5 K with a sweep rate of 3 K/min.

3. Results and discussion

SEM micrographs of the pristine CNT yarns (Fig. 1-a) show that the nanotubes are uniform and predominantly oriented with a helix angle (α) ~25°. SEM micrographs of the chemically prepared CNT-PPy yarn show a non-uniform coating of PPy (Fig. 1-b). Some areas of the Chem. CNT-PPy yarn displayed a surface morphology similar to the surface morphology of the pristine CNT yarn. These areas are labeled A in Fig. 1b. In other parts the surface was less porous, suggesting that the PPy had completely filled the surface pores (Region B in Fig. 1b). The electrochemically developed CNT-PPy yarn shows a core-sheath structure with a CNT inner core (Fig. 1-c). The diameter of the CNT yarns in our experiments, in pristine form, which were also used as the base material for preparing the CNT-PPy yarns, was 10 μm. The diameter of the as-prepared electrochemically and chemically CNT-PPy yarns were 25 and 12 μm, respectively.

Electrical transport of the carbon nanotubes and CNT-PPy yarns was characterized by a standard four probe technique (Quantum Design PPMS). All measured yarns were placed onto MgO substrate and four Au wires were attached sample using silver paste. The dependence of conductivity (σ) on temperature (T) was measured by sweeping the temperature from 350 K to 5 K with a sweep rate of 3 K/min. Fig. 2 compares the temperature dependence of the conductivity and the conductance, $G(T)$, for the pristine CNT yarn as well as the two varieties of CNT-PPy yarns. As can be seen in the inset of Fig. 2, PPy enhances the conductivity of CNT yarns. It is expected that PPy acts as a binder in the PPy-CNT yarn and therefore reduces the slippage between CNT bundles. As a result, the electrical conductivity of the yarn is enhanced due to better connection between CNTs. The conductivity of samples at room temperature was 176, 220, and 235 S/cm, for pristine, electrochemically and chemically prepared materials, respectively. Chemical polymerization of pyrrole could provide the polypyrrole with higher electrical conductivity compared to electrochemically polymerized pyrrole due to its higher molecular weight and longer polymer chain length. The conductance of all samples decreases almost linearly with decreasing temperature down to $T \approx 100$ K and then decreases strongly at lower temperatures. This result is consistent with the behavior observed by other research teams [26]. The resistivity ratio, $\rho_r = \rho(T=5\text{ K})/\rho(300\text{ K})$ was 1.83, 1.7, and 1.72 for the CNT yarn, the electrochemically and chemically prepared CNT-PPy yarn, respectively. Therefore, all samples are certainly in critical regime at temperatures below 100 K because in this region $\rho_r = \rho(T=1.4\text{ K})/\rho(300\text{ K}) < 2$ according to Ref. [24]. The electron transport properties of the conducting yarns at low temperature can be classified in the insulating, critical, or metallic state from the slope of temperature

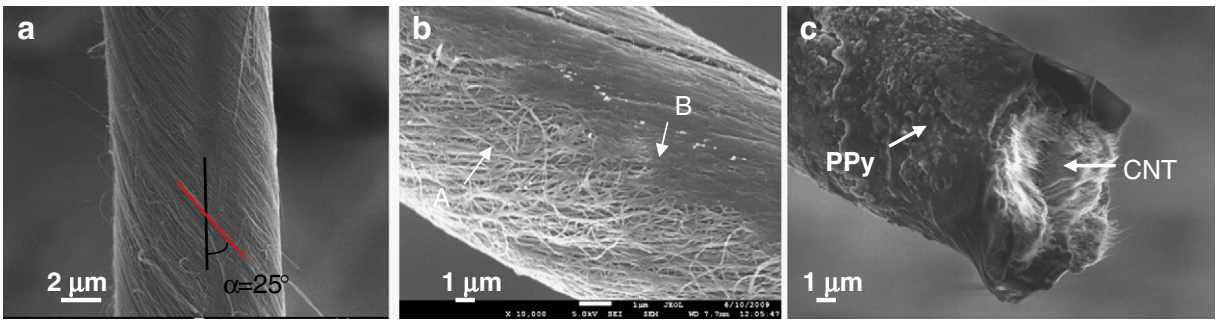

Fig. 1. (a) Pristine CNT yarn, (b) chemical and (c) electrochemical CNT-PPy yarn.

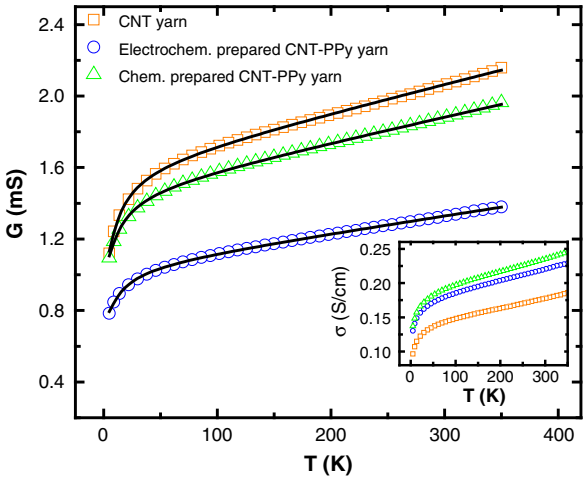

Fig. 2. The temperature dependence of conductance $G(T)$ of the CNT yarn, and chemically and electrochemically prepared CNT-PPy yarns. The solid curves show the two shell model fit to experimental data. Inset: conductivity as a function of temperature for all three samples.

dependence of the reduced activation energy, $W(T)$, which is defined as [27]:

$$W(T) = -\delta\ln(\rho(T))/\delta\ln(T) = \delta\ln(\sigma(T))/\delta\ln(T). \quad (1)$$

Fig. 3 shows a comparison of the $W(T)$ of the pristine CNT yarn and the electrochemically and chemically prepared CNT-PPy yarns. As shown in Fig. 3, at temperatures, lower than 100 K, the $W(T)$ changes slightly with a negative in the slopes. Therefore, the systems are in the critical regime. In this critical region it was found that resistivity (conductivity) follows a power-law as a function of temperature, i.e. [28]:

$$\rho(T) \sim T^{-\beta} \rightarrow \sigma(T) \sim T^{\beta} \quad (2)$$

where the exponent $\beta = W$ at low temperature and varies across the critical regime from 0.3 in the metallic regime side to 1 in the insulating side. As shown in Fig. 3, W is roughly constant for samples with values for β typically falling in the range $0.1 < \beta < 0.2$ at temperatures below 100 K. Therefore, all samples are in the critical regime in the insulator–metal transition, or close to the metallic regime.

For tested samples, the temperature dependence of the conductivity of yarns is explained at $T < 100$ K by Mott's law, which is the exponential temperature dependence characteristic of variable range hopping (VRH) model [29]:

$$\sigma(T) = \sigma_0 \exp\left[\left(-\frac{T_0}{T}\right)^{1/(1+d)}\right] \quad (3)$$

where σ_0 is the high temperature limit of DC conductivity, T_0 is related to thermally activated hopping among localized states and d is the dimensionality of the conduction process. The dimensionality, d, could take values between one and three, showing one, two or three dimensional conduction characteristics.

Fig. 4 shows $\ln \sigma(T)$ vs. $T^{-1/(1+d)}$ with $d = 3$ at low temperatures, i.e. $T < 100$ K, for the pristine CNT yarn and the electrochemically and chemically prepared CNT-PPy yarns. The conductivity is evaluated from the best-fitted straight lines as presented in Fig. 4. These results support the hypothesis that the transport mechanisms correspond to a 3D-VRH model in all three types of yarn samples. The best-fitted values of T_0, which can be interpreted as the effective energy separation between localized states, and σ_0 for 3D-VRH model, are shown in Table 1 for the three samples. The results show that T_0 for the CNT yarn (2.14 K) is larger than that for both the electrochemically and chemically prepared CNT-PPy yarn ($\approx$1.1 K) by a factor of almost 2. Therefore, the effective energy separations between localized states of the electrochemically and chemically prepared CNT-PPy yarn samples are smaller than pristine yarn. This is supported by higher σ_0 values.

The T_0 for 3D-VRH is given by:

$$T_0 = \frac{16}{k_B L^3 N(E_F)} \quad (4)$$

where L is the localization length and $N(E_F)$ is the density of states at the Fermi level. Disorder degrees of systems decrease with lowering T_0 because T_0 is inversely proportional to L. The values of L are calculated by considering the charge transport primarily arising from the conducting phase and assuming $N(E_F)$ of about 7.5×10^{19} eV^{-1} cm^{-3} as reported in Aggarwal et al. [30] and De et al. [31]. The localization length, L, values are shown in Table 1 for the three samples. The localization length for the CNT yarn is about 105 nm, while for the both CNT-PPy yarns it increases to about 130 ± 2 nm. The average hopping distance R_{hop} between two sites and the activation energy, W_{hop}, are given by:

$$R_{hop} = \frac{3}{8}\left(\frac{T_0}{T}\right)^{1/4} L \quad (5)$$

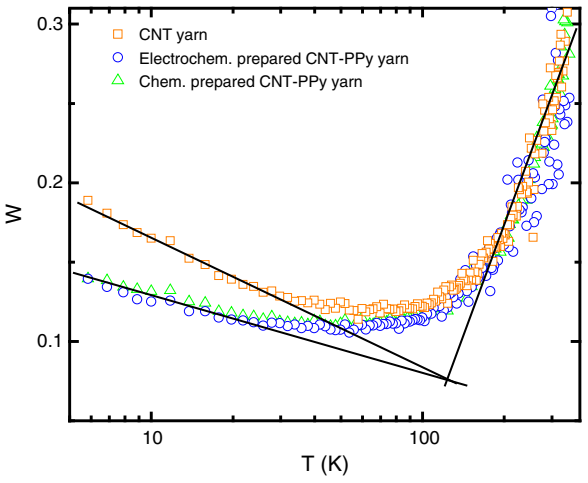

Fig. 3. Temperature dependence of reduced activation energy $W(T)$ of the CNT yarn, and electrochemically and chemically prepared CNT-PPy yarns.

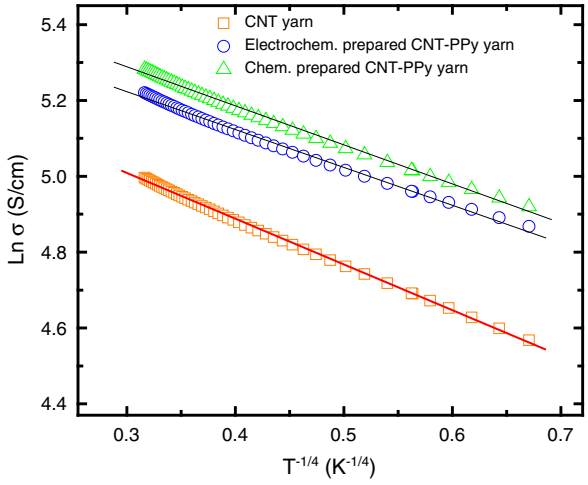

Fig. 4. Three dimensional VRH (3D-VRH) model ($\ln \sigma(T)$ vs. $T^{-1/(1+d)}$ with $d = 1$ $d = 3$ at low temperatures, i.e. $T < 100$ K) for the CNT yarn and electrochemically and chemically prepared CNT-PPy yarns.

Table 1
Conductivity analysis for the 3 CNT yarn test samples.

Sample	T_0 (K)	σ_0 (S/cm)	L (nm)	R_{hop} (nm)	W_{hop} (meV)
CNT yarn	2.14	215.1	105	11.5	1.88
Electrochemical CNT-PPy yarn	1.05	252.0	133	12.2	1.57
Chemical CNT-PPy yarn	1.18	270.8	128	12.0	1.62

$$W_{hop} = \frac{1}{4} k_B T \left(\frac{T_0}{T}\right)^{1/4}. \quad (6)$$

At room temperatures, the average hopping distance for the CNT yarn is about 11.5 nm while for both CNT-PPy yarns it increases to about 12 nm. These distances correspond to about 35–40 pyrrole monomer units in length. The estimated activation energies for hopping are 1.88 meV and ≈1.60 meV for the CNT yarn and CNT-PPy yarn, respectively (as shown in Table 1). MWNT are almost guaranteed to have metallic behavior but when short pieces of MWNT are integrated into a yarn they will not act as stretched uninterrupted paths for electrons. Instead, electrons could use the uninterrupted short path of a single piece of MWNT and then progress to another adjacent piece of MWNT and so on.

Based on the electrical conductivity relationship with temperature fitting the One Dimensional VRH (1D-VRH), it has already been shown that 1D-VRH conduction is the dominant electron transfer mechanism in disordered MWNT [32]. CNT yarns, regardless of being pristine or composite, are predominantly made of a group of MWNTs that are aligned, packed, and follow each other back to back using van der Waals interaction. One can then regard these elongated back to back strands of MWNTs as disordered MWNTs. Therefore, the observed behavior can be explained and appears realistic. In addition, given that at the ends of every piece of MWNT in the yarn the electrons have the likelihood of switching direction and moving to other nearby strands of MWNTs, this can explain the three dimensional characteristic of the fitting model.

Another model, called the two shell model, was suggested to explain the electronic transport of MWNTs by Skákalová et al. [33]. They proposed that thermally assisted transfer of electrons from the outer shell to the inner shell and the activated or fluctuation-assisted tunneling [33] current through the inner shell are two main mechanisms for flowing of current through MWNTs. Based on the two shell model, the conductance is given by:

$$G(T) = G_1 + G_{20} \exp\left(-\frac{T_b}{T + T_S}\right) \quad (7)$$

where $G1 = G_{10} + AT$ to incorporate a term increasing linearly with temperature T due to the conductance of the outer shell between the voltage electrodes. T_b is the order of magnitude of typical barrier energies indicated by the value of $k_B T_b$ and the ratio T_s/T_b shows the decrease of conductivity at low temperatures. As can be seen in Fig. 2, this expression (Eq. (7)) gives a very good description of the conductance T dependence for the CNT yarn and the electrochemically and chemically prepared CNT-PPy yarn. The best fitted values of two shell model parameters are shown in Table 2 for all samples. The fitted value of the activation energy $k_B T$ was 0.99, 1.08, and 1.15 meV ($T_b = 11.5$, 12.6, and 13.3 K) for the CNT yarn, the chemically prepared CNT-PPy and the electrochemically yarn, respectively. For all samples, the parameter T_s was zero, i.e., a simple activated form was adequate to describe the nonlinear temperature dependence.

Table 2
Conductance analysis based on two shell model for the CNT yarn, the chemically prepared CNT-PPy, and the electrochemically yarn.

Sample	G_{10} (mS)	A (μS/K)	G_{20} (mS)	T_b (K)
CNT yarn	1.07	1.56	0.55	11.5
Chemically CNT-PPy yarn	1.07	1.39	0.41	12.6
Electrochemically CNT-PPy yarn	0.77	0.96	0.28	13.3

4. Conclusions

In this work, three types of pristine and carbon nanotube-polypyrrole composite yarns were compared in terms of electron transport. The results suggest that the electron transport in all of these yarns is consistent with a three dimensional hopping mechanism. This behavior is most likely due to the defect structures of CNT composites, in which electrons cannot be confined in the one-dimensional channel along the CNT aligned direction. Instead, electrons hop from one localized site to another or from one CNT to another. The effective energy separation between localized states of the pristine CNT yarn is larger than that for both the electrochemically and chemically prepared CNT-PPy yarns. All three yarns show critical behavior in the insulator–metal transition, or close to the metallic regime at low temperature. The 3D-VRH model has been validated for CNT yarn in both pristine and composite forms. It may be speculated that any other CNT yarn composite, with a sizeable CNT component, should also show the same attributes but this requires confirmation. It was found that the two shell model accurately describes our data in the temperature range of 5 to 350 K.

Acknowledgments

The authors would like to thank Professor Ray Baughman (University of Texas at Dallas) for his continuous support, insights and also for providing the CNT forests needed for producing the yarns.

References

[1] Y.-L. Li, I.A. Kinloch, A.H. Windle, Science 304 (2004) 276.
[2] M. Zhang, K.R. Atkinson, R.H. Baughman, Science 306 (2004) 1358.
[3] W. Zhou, J. Vavro, C. Guthy, K.I. Winey, J.E. Fischer, L.M. Ericson, S. Ramesh, R. Saini, V.A. Davis, C. Kittrell, M. Pasquali, R.H. Hauge, R.E. Smalley, J. Appl. Phys. 95 (2004) 649.
[4] H.W. Zhu, C.L. Xu, D.H. Wu, B.Q. Wei, R. Vajtai, P.M. Ajayan, Science 296 (2002) 884.
[5] L. Zhu, J. Xu, Y. Xiu, Y. Sun, D.W. Hess, C.P. Wong, Carbon 44 (2006) 253.
[6] H. Dai, Acc. Chem. Res. 35 (2002) 1035.
[7] P.L. McEuen, J.Y. Park, MRS Bull. 29 (2004) 272.
[8] A.P. Ramirez, Bell Labs Tech. J. 10 (2005) 171.
[9] R.H. Baughman, C. Cui, A.A. Zakhidov, Z. Iqbal, J.N. Barisci, G.M. Spinks, G.G. Wallace, A. Mazzoldi, D. De Rossi, A.G. Rinzler, O. Jaschinski, S. Roth, M. Kertesz, Science 284 (1999) 1340.
[10] J. Foroughi, G.M. Spinks, G.G. Wallace, J. Oh, M.E. Kozlov, S. Fang, T. Mirfakhrai, J.D.W. Madden, M.K. Shin, S.J. Kim, R.H. Baughman, Science 334 (2011) 494.
[11] J.G. Park, G.T. Kim, J.H. Park, H.Y. Yu, G. McIntosh, V. Krstic, S.H. Jhang, B. Kim, S.H. Lee, S.W. Lee, M. Burghard, S. Roth, Y.W. Park, Thin Solid Films 393 (2001) 161.
[12] A. Bachtold, M. Henny, C. Terrier, C. Strunk, C. Schonenberger, J.P. Salvetat, J.M. Bonard, L. Forro, Appl. Phys. Lett. 73 (1998) 274.
[13] C. Berger, Y. Yi, Z.L. Wang, W.A. de Heer, Appl. Phys. A: Mater. Sci. Process. 74 (2002) 363.
[14] B. Gao, Y.F. Chen, M.S. Fuhrer, D.C. Glattli, A. Bachtold, Phys. Rev. Lett. 95 (2005) 196802.
[15] P.L. McEuen, M.S. Fuhrer, P. Hongkun, IEEE Trans. Nanotechnol. 1 (2002) 78.
[16] H.J. Dai, E.W. Wong, C.M. Lieber, Science 272 (1996) 523.
[17] S.N. Song, X.K. Wang, R.P.H. Chang, J.B. Ketterson, Phys. Rev. Lett. 72 (1994) 697.
[18] Q. Li, Y. Li, X. Zhang, S.B. Chikkannanavar, Y. Zhao, A.M. Dangelewicz, L. Zheng, S.K. Doorn, Q. Jia, D.E. Peterson, P.N. Arendt, Y. Zhu, Adv. Mater. 19 (2007) 3358.
[19] N. Ferrer-Anglada, M. Kaempgen, V. Skákalová, U. Dettlaf-Weglikowska, S. Roth, Diam. Relat. Mater. 13 (2004) 256.
[20] S.H.M. Persson, P. Dyreklev, O. InganÃs, Adv. Mater. 8 (1996) 405.
[21] V. Gomis, D. Bellver, N. Ferrer-Anglada, J.M. Ribó, Z. El-Hachemi, B. Movaghar, Synth. Met. 156 (2006) 1083.
[22] J.G. Park, G.T. Kim, V. Krstic, B. Kim, S.H. Lee, S. Roth, M. Burghard, Y.W. Park, Synth. Met. 119 (2001) 53.
[23] A.B. Kaiser, Y.W. Park, Curr. Appl. Phys. 2 (2002) 33.

[24] J. Foroughi, S.R. Ghorbani, G. Peleckis, G.M. Spinks, G.G. Wallace, X.L. Wang, S.X. Dou, J. Appl. Phys. 107 (2010) 103712.
[25] J. Foroughi, Development of Novel Nanostructured Conducting Polypyrrole Fibres in Engineering, Univ. of Wollongong, Wollongong, Australia, 2009.
[26] A.E. Aliev, C. Guthy, M. Zhang, S. Fang, A.A. Zakhidov, J.E. Fischer, R.H. Baughman, Carbon 45 (2007) 2880.
[27] R. Menon, C.O. Yoon, D. Moses, A.J. Heeger, Y. Cao, Phys. Rev. B 48 (1993) 17685.
[28] C.O. Yoon, R.M.D. Moses, A.J. Heeger, Phys. Rev. B 49 (1994) 10851.
[29] N.F. Mott, E. Davis, Electronic Process in Non-Crystalline Materials, 2nd ed. Oxford, Clarendon, 1979.
[30] M. Aggarwal, S. Khan, M. Husain, T.C. Ming, M.Y. Tsai, T.P. Perng, Z.H. Khan, Eur. Phys. J. B. 60 (2007) 319.
[31] S. De, A. Dey, S.K. De, Solid State Commun. 137 (2006) 662.
[32] D.P. Wang, D.E. Feldman, B.R. Perkins, A.J. Yin, G.H. Wang, J.M. Xu, A. Zaslavsky, Solid State Commun. 142 (2007) 287.
[33] V. Skákalová, A.B. Kaiser, Y.S. Woo, S. Roth, Phys. Rev. B 74 (2006) 085403.